

Dielectric, ferromagnetic and ferroelectric properties of the $(1 - x)\text{Ba}_{0.8}\text{Sr}_{0.2}\text{TiO}_3-x\text{CoFe}_2\text{O}_4$ multiferroic particulate ceramic composites

Yean Wang · Yunbo Wang · Wei Rao ·
Meng Wang · Gangxian Li · Yubin Li ·
Junxiong Gao · Wenli Zhou · Jun Yu

Received: 12 July 2011 / Accepted: 11 October 2011 / Published online: 20 October 2011
© Springer Science+Business Media, LLC 2011

Abstract The $(1 - x)\text{Ba}_{0.8}\text{Sr}_{0.2}\text{TiO}_3-x\text{CoFe}_2\text{O}_4$ ceramic composites ($x = 0-1$) were prepared by standard solid state reaction method. X-ray diffraction and SEM indicate the $\text{Ba}_{0.8}\text{Sr}_{0.2}\text{TiO}_3$ (BST) phase and CoFe_2O_4 (CFO) phase coexist in the composites. The dielectric constant and dielectric loss for the composites were studied as a function of frequency (40 Hz–1 MHz) and temperature (30–600 °C). Magnetic and ferroelectric tests show that the ceramic composites display ferromagnetic and ferroelectric properties simultaneously. The saturated polarization of the composites decrease with ferrite concentration increasing, while the remnant polarization of the composites increase with increasing ferrite concentration. The enhanced ferroelectricity of composites may be attributed to space charge contribution in the composites.

1 Introduction

Multiferroic magnetoelectric (ME) materials not only exhibit ferroelectric and ferromagnetic properties simultaneously, but also exist the coupling effect which is a dielectric polarization induced by an external magnetic field or a magnetization induced by an applied electric field [1]. Recently, ME materials have been attracting considerable attention for their potential applications in new memories, sensors, transducers etc. [2]. Up to now, magnetoelectric coupling effects have been observed both in single phase

compounds and composite materials. However, the magnetoelectric coupling effects in single phase compounds are considerably weak even at low temperatures, thus their applications for practical devices are limited [3]. More and more researchers have paid attention to the magnetoelectric composites consisting of ferroelectric phase and ferromagnetic phase [4, 5]. The magnetoelectric effects are originated from the magnetic-mechanical-electric interaction between ferroelectric and ferromagnetic phase. When an external magnetic field is applied to the composites, the ferrite particles change their shape due to magnetostrictive effect, and then the produced strain passes to the piezoelectric phase, resulting in an electric polarization due to piezoelectric effect [6]. Barium strontium titanate (BaSrTiO_3) has been considered to be an important material for tunable microwave devices due to its superior dielectric constant, large electric field tunability, relatively low dielectric loss and variable Curie temperature (from 400 to 30 K) depending on the content of strontium [7, 8]. Cobalt ferrite (CoFe_2O_4) has high resistivity and large magnetostrictive coefficient [9]. Although, $(1 - x)\text{Ba}_{0.8}\text{Sr}_{0.2}\text{TiO}_3-x\text{CoFe}_2\text{O}_4$ multiferroic particulate ceramic composites have been reported by Kanamadi et al. [10, 11], the research for these composites is very rare. So in order to improve their dielectric and multiferroic properties, further investigations on them under different fabrication procedures and processing parameters are needed. Moreover, the ferroelectric properties of these composites have not been reported so far [10, 11], it is very significant to study ferrite concentration dependence of ferroelectric properties.

In this paper, $(1 - x)\text{Ba}_{0.8}\text{Sr}_{0.2}\text{TiO}_3-x\text{CoFe}_2\text{O}_4$ ceramic composites with $x = 0-0.4$ and 1, respectively were prepared by standard solid state reaction method. The influences of ferrite concentration on the dielectric, ferromagnetic and ferroelectric properties were investigated.

Y. Wang · Y. Wang (✉) · W. Rao · M. Wang · G. Li · Y. Li ·
J. Gao · W. Zhou · J. Yu
Department of Electronic Science and Technology, Huazhong
University of Science and Technology, Wuhan 430074, China
e-mail: ybwang2011@126.com

2 Experiments

The $(1-x)\text{Ba}_{0.8}\text{Sr}_{0.2}\text{TiO}_3-x\text{CoFe}_2\text{O}_4$ ceramic composites with $x = 0.1-0.4$ were prepared by standard solid state reaction method. The starting powders of BaCO_3 , SrCO_3 and TiO_2 (purity $\geq 99.0\%$) were weighed exactly in stoichiometric proportion. The mixtures were thoroughly mixed in an agate mortar with alcohol and then ground for about 12 h, then presintered at 950°C for 2 h and subsequently ground again in the agate mortar for 12 h. The ferromagnetic phase was prepared by mixing the starting powders of Co_2O_3 and Fe_2O_3 (purity $\geq 99.0\%$) in stoichiometric proportion and thoroughly mixed in an agate mortar with alcohol, then ground for about 12 h and presintered at 900°C for 2 h. The $(1-x)\text{Ba}_{0.8}\text{Sr}_{0.2}\text{TiO}_3-x\text{CoFe}_2\text{O}_4$ composites were fabricated by mixing 10, 20, 30 and 40 mol% of ferromagnetic phase with 90, 80, 70 and 60 mol% of ferroelectric phase, respectively. The composites were ground for about 12 h, then presintered again at 1100°C for 2 h, subsequently ground again for 12 h. The slurry was dried and ground with polyvinyl alcohol (PVA), then pressed into discs with the dimensions of 20 mm in diameter and 1.2 mm in thickness. Finally, the discs were sintered at 1300°C for 2 h in air.

The phase structures of the composites were characterized by X-ray diffraction (XRD) (X'Pert PRO, PANalytical B.V.) with Cu K_α radiation ($\lambda = 1.5406 \text{ \AA}$). To study the morphology of the composites, Scanning Electron Microscope (SEM, Quanta 200) was used to observe the surface topography. The densities of the composites were measured using Archimedeian method. The resistivity of the composites was evaluated by multimeter at room temperature. The dielectric properties with frequency in the range of 40 Hz–1 MHz at room temperature were measured using precise impedance analyzer (Agilent 4294A). The dielectric constant and dielectric loss as a function of temperature at different frequencies were measured using precise impedance analyzer (HP4284A). Magnetic measurements were studied at room temperature using vibrating sample magnetometer (VSM, LakeShore 7404). Ferroelectric properties were carried out using ferroelectric tester (PremierII, Radiant Technologies) in silicon oil at room temperature. For the measurements of electrical properties, the composite discs were carefully polished and then covered with silver paste on both sides as electrodes, which were finally dried for 20 min.

3 Results and analysis

Figure 1 shows the XRD patterns of the composites. It can be seen that pure CFO ceramic has single-phase cubic spinel structure, pure BST ceramic has single-phase

tetragonal perovskite structure, and Other composites with $x = 0.1-0.4$ are, respectively composed of tetragonal perovskite BST phase and cubic spinel CFO phase, without other intermediate phase or impurity phase. The intensity of BST peaks decreases with decrease in BST concentration in the composites. The lattice constant for ferrite phase in composite with 20% ferrite concentration is $a = 8.366 \text{ \AA}$, and the ones for ferroelectric phase are $a = 3.982 \text{ \AA}$ and $c = 3.990 \text{ \AA}$ ($c/a = 1.002$).

The variations of densities and DC resistivity of the composites with ferrite concentration are shown in Fig. 2, respectively. The respective densities of the composites with $x = 0.1-0.4$ are 5.31, 5.10, 5.08 and 5.01 g/cm^3 . The densities decrease with increasing the ferrite concentration. The resistivity of the composites with $x = 0.1-0.4$ is 4.7×10^8 , 1.1×10^8 , 5.9×10^7 and $3.6 \times 10^7 \text{ }\Omega\text{cm}$, respectively. The resistivity of the composites decreases with the increase in ferrite concentration, which is due to the increasing concentration of ferrite phase with low resistivity.

The backscattered SEM micrographs of the composites are shown in Fig. 3. It indicates all the composites show dense microstructure, less pores and no cracks, as well as BST phase and CFO phase coexist in the composites, in which the BST phase appears as white area and CFO phase appears as black area. The dark area increases with increasing CFO concentration. At $x = 0.2$, the spinel CFO grains are comparatively well dispersed in the perovskite BST matrix. With x increasing to 0.3 and 0.4, the some isolated spinel CFO grains begin to aggregate.

Figure 4 displays the leakage current density–electric field (J–E) behavior of the composites. With increasing ferrite concentration, the leakage current densities of composites increase. At an applied electric field of 10 kv/cm ,

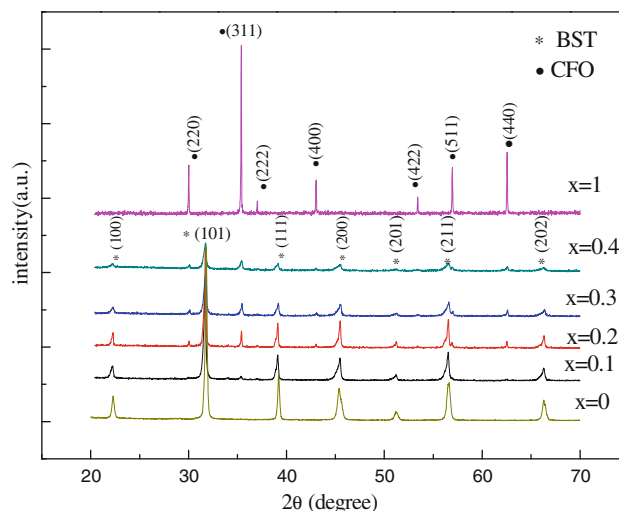


Fig. 1 XRD patterns of the $(1-x)\text{BST}-x\text{CFO}$ ceramic composites with $x = 0-0.4$ and 1

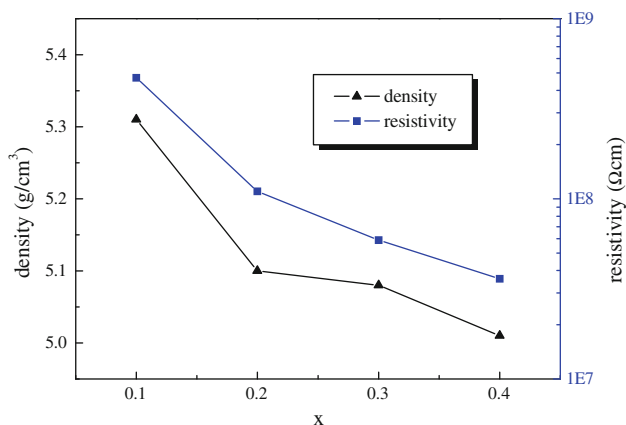


Fig. 2 The ferrite concentration dependence of the densities and resistivity for composites

the leakage current densities of composites with $x = 0.1$ – 0.4 are 4.4×10^{-5} , 1.0×10^{-4} , 1.7×10^{-4} , and 2.6×10^{-4} A/cm², respectively. Due to the comparatively low resistivity of ferrite phase, as the ferrite concentration in the composites increases, the aggregation of ferrite phase, which is demonstrated in the above SEM micrographs, leads to the decrease of composites resistivity.

The variations of dielectric constant (ϵ_r) and dielectric loss ($\tan\delta$) with frequency in the range of 40 Hz–1 MHz for the composites at room temperature are shown in Fig. 5. Ba_{0.8}Sr_{0.2}TiO₃ has comparatively high permittivity, while CoFe₂O₄ is a low dielectric constant material. From the Fig. 5a, the dielectric constant of composites decreases with increase in ferrite concentration, as expected. The decrease in dielectric constant may be ascribed to the decrease of composites resistivity as the ferrite concentration increases. The dielectric constant values of composites with $x = 0.1$ – 0.4 are 1498.2, 966.5, 601.0, and 384.6 at 1 MHz, respectively. It can be seen that the dielectric constant rapidly decreases with increase in frequency at lower frequency showing dielectric dispersion and then reaches to a fairly constant at higher frequency. The high value of dielectric constant observed at lower frequency was explained on the basis of space charge polarization due to inhomogeneous dielectric structure and resistivity of the samples [12]. The dielectric dispersion at lower frequency can be explained on the basis of Koop's phenomenological theory and Maxwell–Wagner interfacial polarization theory [13–15]. Since an assembly of space charge carriers in the inhomogeneous dielectric structure described requires finite time to line up their axis parallel to an alternating electric field, the dielectric constant naturally decreases, if the frequency of the reversal field increases [16].

Figure 5b shows that dielectric loss increases firstly to a peak with increase in frequency and then decreases at lower frequency, which presents dielectric dispersion. The

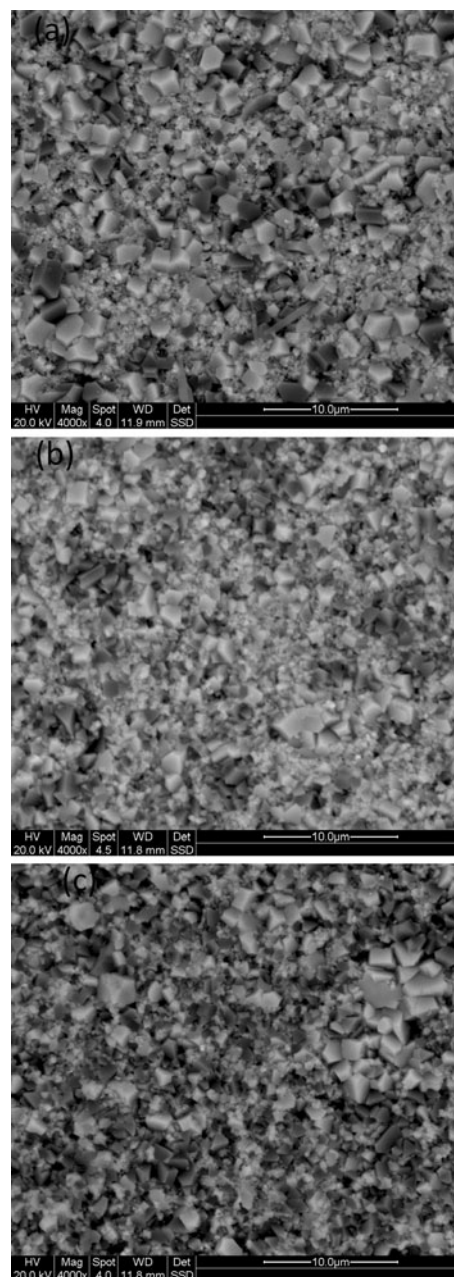


Fig. 3 Backscattered SEM micrographs of the $(1-x)$ BST- x CFO composites with $x = 0.2$ (a), $x = 0.3$ (b) and $x = 0.4$ (c)

dielectric dispersion at lower frequency can be explained by Maxwell–Wagner interfacial polarization theory [14, 15]. It was reported by Zhang et al. [17] that they used Maxwell–Wagner space charge model to calculate in comparison with the experimental observation and concluded that the peak of dielectric loss at a relatively low frequency should be originated from the space charge effect in the PZT/CFO multilayer capacitors. In addition, it can be further observed that the dielectric loss increases as ferrite concentration increases. The dielectric loss values of the composites with $x = 0.1$ – 0.4 are 0.0055, 0.0068,

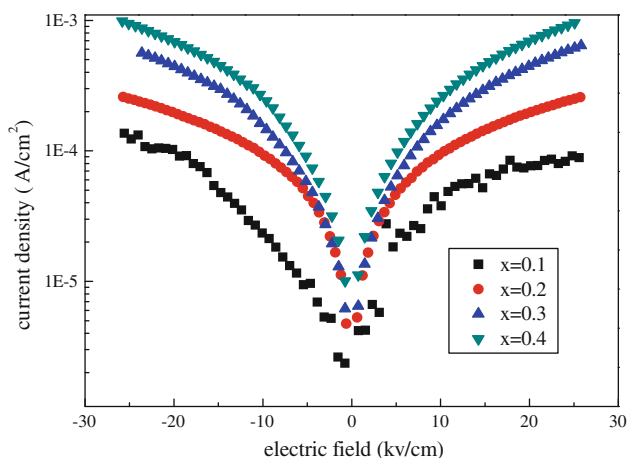


Fig. 4 The leakage current density–electric field (J–E) behavior of the $(1 - x)\text{BST}-x\text{CFO}$ composites with $x = 0.1-0.4$

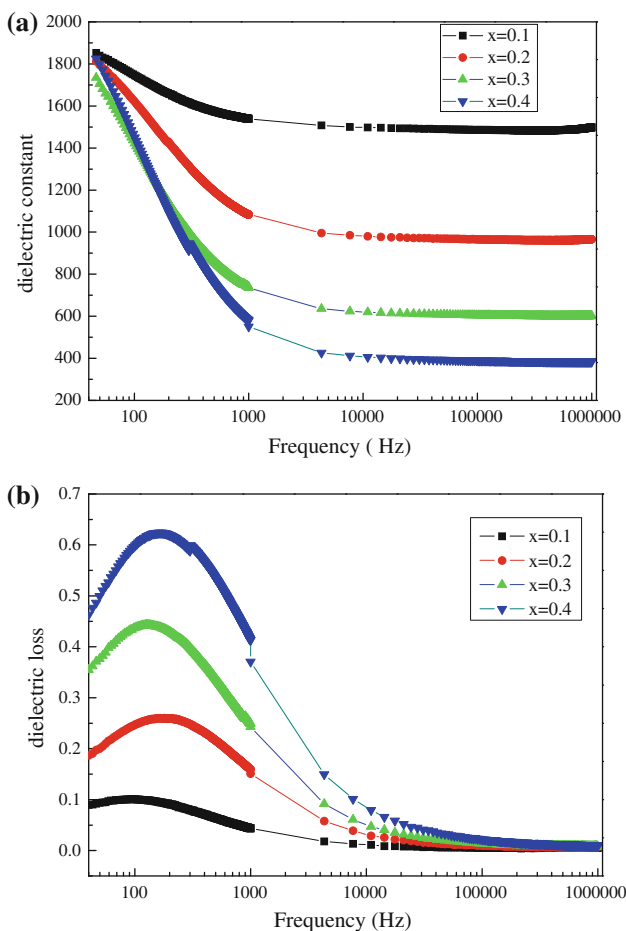


Fig. 5 Variation of dielectric constant (a) and dielectric loss (b) with frequency for the $(1 - x)\text{BST}-x\text{CFO}$ composites with $x = 0.1-0.4$

0.0078 and 0.0093 at 1 MHz, respectively. By close observation on Fig. 5, one can find a small kink of sample $x = 0.4$ on both dielectric constant and dielectric loss at the lower frequency. When $x = 0.4$ in composite, it is likely

for Co^{2+} and (or) Fe^{3+} to enter into the A and B sites of $\text{Ba}_{0.8}\text{Sr}_{0.2}\text{TiO}_3$ in composite more easily, resulting in the disorder in the arrangement of the Sr and Ba cations. At lower frequency, the dipolar and space charge contribute to the dielectric polarization dominantly. The dipolar and space charge polarization have a small kink at the lower frequency, which may be ascribed to the disorder in the arrangement of the Sr and Ba cations.

The Fig. 6a–d shows temperature dependence of dielectric constant for the composites at different frequencies. The dielectric constant increases with the increase in temperature up to the ferroelectric Curie temperature (T_c) and then decreases, indicating ferroelectric phase transition. It can be also seen that the T_c shifts toward higher temperature as the frequencies increase. These composites exhibit diffused phase transition (DPT), showing the typical characteristics of relaxor ferroelectrics. From the plot, it also indicates the T_c decreases slightly with increasing ferrite concentration. In addition, it is found that the dielectric constant decreases with the increase in ferrite concentration in the composites. The decrease in dielectric constant is attributed to the incorporation of ferrite phase with low dielectric constant into the ferroelectric matrix. It is reported that different behavior of permittivity as a function of compositions is a result of two effects, modification of the piezoelectric material with ferrite components and change in grain size of piezoelectric materials [18].

The high value of dielectric constant is attributed to the following two reasons. The one is that it is due to the electronic hopping between Fe^{3+} and Fe^{2+} ions and hole hopping between Co^{2+} and Co^{3+} ions in the spinel structure. In spinel ferromagnetic CoFe_2O_4 , the Co^{2+} and Fe^{3+} ions are not only restricted in tetrahedral and octahedral sites, respectively, but also Co ion occupies the octahedral sites and Fe ions the tetrahedral sites, thus resulting in the hopping of charge carriers. The charge carriers cause local displacement along the direction of the electric field, resulting in dielectric polarization in ferrites. The other is the influence of space charges at the interfaces between the ferroelectric and ferromagnetic phases.

For the composites with $x = 0.1$ and 0.2 , it is observed that the dielectric constant increase as the temperature increases above phase transition temperature at the lower frequency range. At lower frequency, the dipolar and space charge polarizations contribute to the dielectric constant dominantly. These space charges gain higher mobility as the frequency lowers or the temperature increases, thus leading to the increasing dielectric constant continuously. While for the composites with $x = 0.3$ and 0.4 , the phenomenon is not observed, which may be resulted from the increasing concentration of ferrite phase with low dielectric constant.

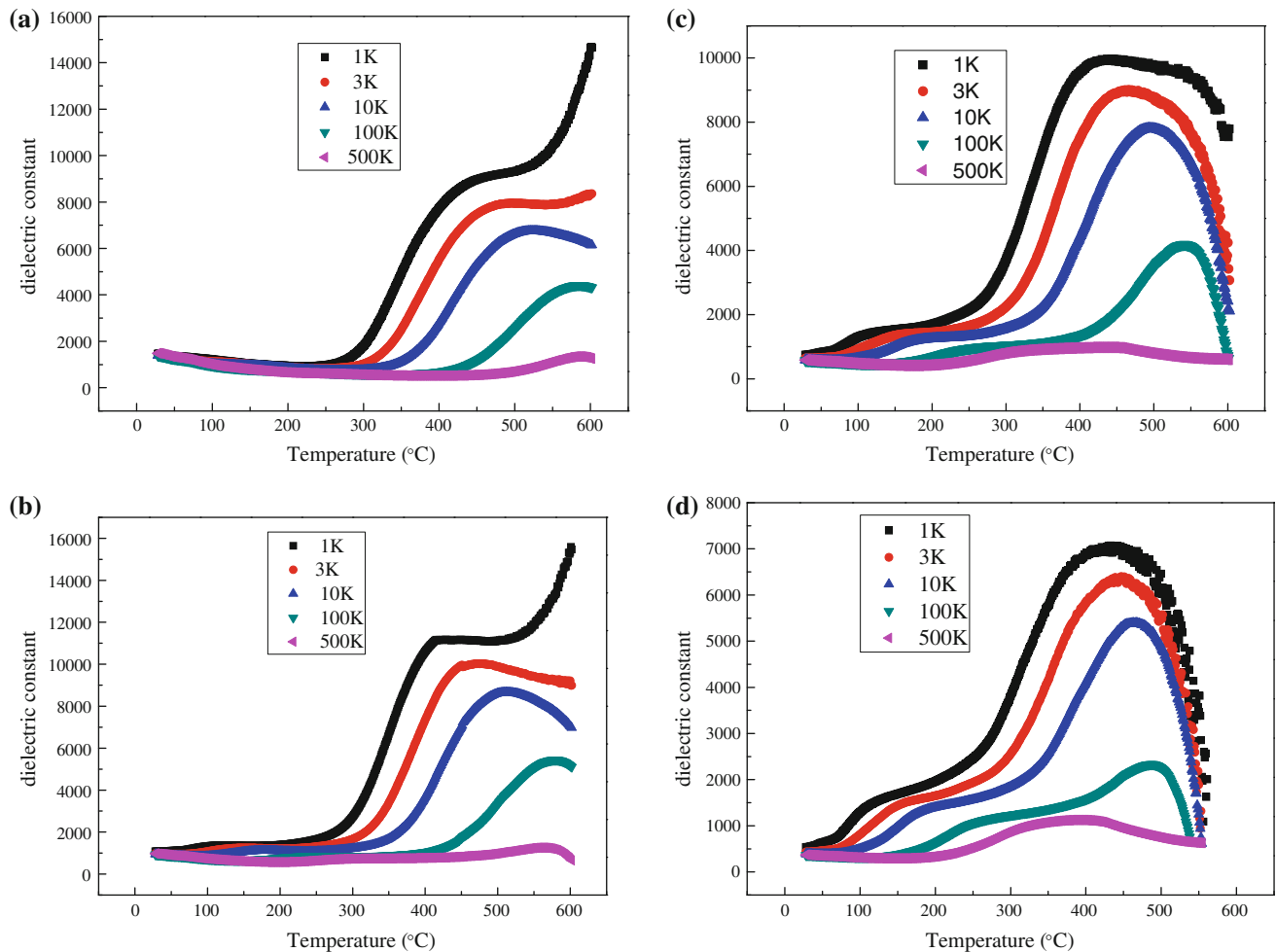


Fig. 6 The variation of dielectric constant with temperature at different frequencies for the $(1-x)\text{BST}-x\text{CFO}$ composites with **a** $x = 0.1$, **b** $x = 0.2$, **c** $x = 0.3$ and **d** $x = 0.4$

The variation of dielectric loss with temperature for the composites with $x = 0.1$ and 0.2 at the different frequencies is shown in Fig. 7a, b. It can be seen that the broaden peaks also exhibit the composites behave as relaxor ferroelectrics.

The variation of magnetization as a function of magnetic field is shown in Fig. 8 for the composites at the maximum applied magnetic field of 15 kOe. The hysteresis loops show all the composites display ferromagnetic characteristics. The saturation magnetization (M_s) values of the composites with $x = 0.1-0.4$ and 1 are 7.02, 18.54, 32.14, 43.53 and 113.17 emu/g, respectively. The remnant magnetization (M_r) values of the composites with $x = 0.1-0.4$ and 1 are 1.62, 4.14, 7.82, 10.68 and 10.53 emu/g, respectively. The M_s values of the composites increase almost linearly with increasing ferrite concentration, as shown in Fig. 9, which displays the ferromagnetic property of the composites is diluted with increasing the concentration of ferroelectric phase. The coercive field (H_c) values of the composites with

$x = 0.1-0.4$ and 1 are 279.18, 320.97, 400.59, 481.55 and 256.17 Oe, respectively. The H_c values of the composites are all larger than that of pure CoFe_2O_4 bulk ceramic, indicating magnetic domain wall motion and rotation become harder in the composites than those in the CoFe_2O_4 bulk ceramic. On the other hand, the H_c values of the composites increase with increasing ferrite concentration, revealing magnetization becomes harder with increasing ferrite concentration. This variation of coercive field may be ascribed to the following two factors. One is the change in the total magnetocrystalline anisotropy energy related to the ME coupling due to the compressive stress in the CFO phase caused by the lattice mismatch between the CFO and BST phases [19]. The other is that the CFO particle size and particle distribution in composites compared to those of pure CFO bulk can affect the coercive field [20].

Figure 10a–e shows polarization–electric field hysteresis loops of the composites, which indicate all the composites demonstrate ferroelectric characteristics. The CFO

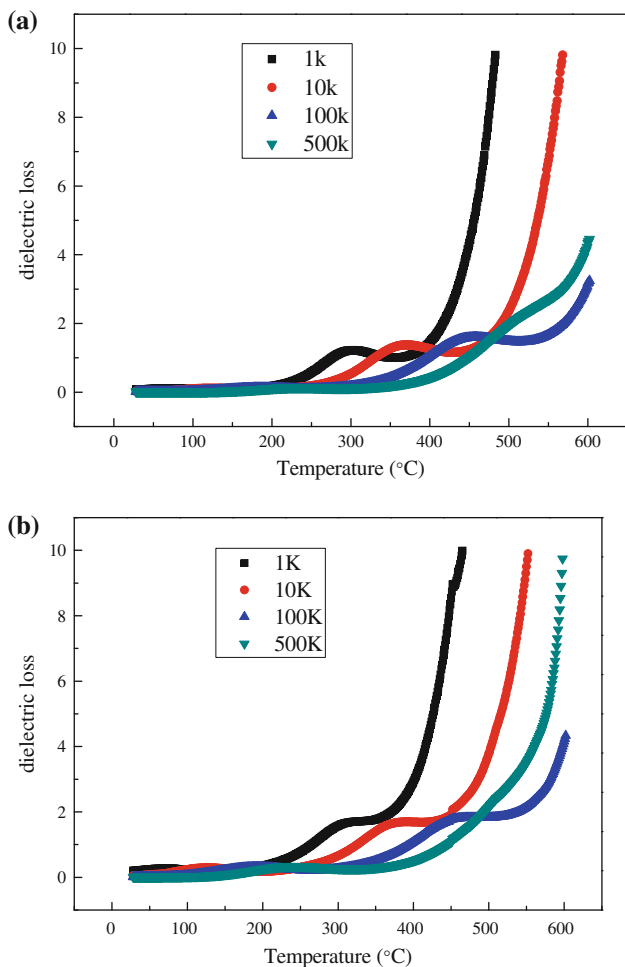


Fig. 7 The variation of dielectric loss with temperature at different frequencies for the composites with **a** $x = 0.1$ and **b** $x = 0.2$

concentration dependence of the remanent and saturated polarization for the composites is shown in Fig. 11. The saturated polarization ($2P_s$) values of the composites with $x = 0-0.4$ are 29.4, 12.4, 10.6, 9.7 and 8.6 $\mu\text{C}/\text{cm}^2$, respectively. The $2P_s$ values decrease with increasing ferrite concentration. The remnant polarization ($2P_r$) values of the composites with $x = 0-0.4$ are 7.1, 3.0, 4.6, 8.4 and 8.7 $\mu\text{C}/\text{cm}^2$, respectively. In comparison with the pure BST ceramic, the $2P_s$ values of the composites with $x = 0.1-0.4$ are smaller than that of the pure BST ceramic, respectively. Meanwhile, the $2P_s$ values of the composites decrease with the increase in ferrite concentration. The reason for the phenomenon is that increasing ferrite concentration can dilute the ferroelectric properties, which is consistent with the other reports [21, 22]. The coercive field ($2E_c$) values of the composites with $x = 0-0.4$ are 5.47, 12.03, 22.08, 36.37 and 39.67 kV/cm , respectively. The $2E_c$ values of the composites with $x = 0.1-0.4$ are larger than that of the pure BST ceramic and increase with increasing ferrite concentration, which is due to the hindered and pinned

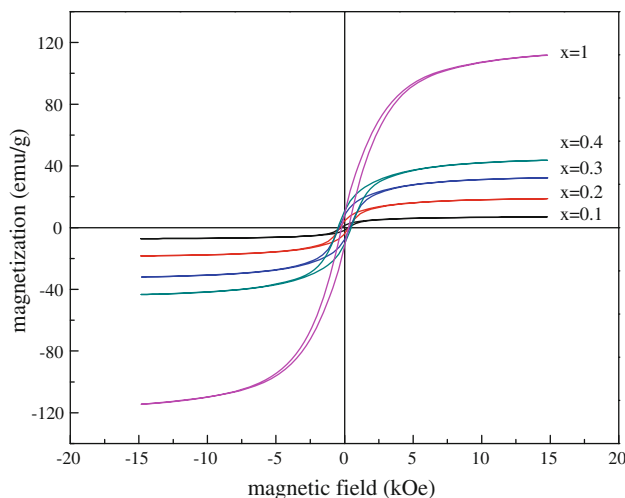


Fig. 8 The ferromagnetic hysteresis loops of the $(1-x)\text{BST}-x\text{CFO}$ composites with $x = 0.1-0.4$ and 1 at room temperature

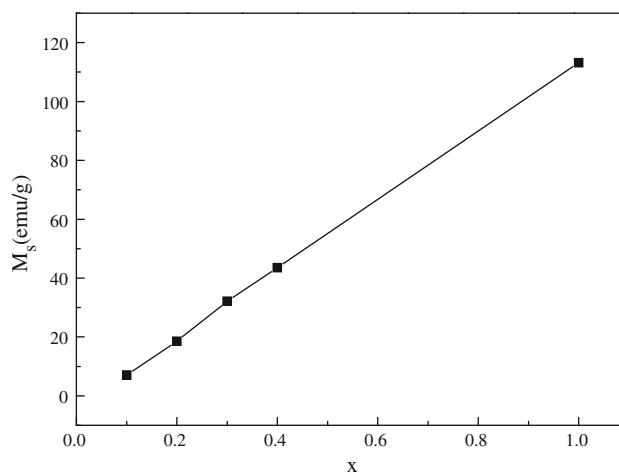


Fig. 9 CFO concentration dependence of the M_s patterns for composites

domain wall motion of ferroelectric regions due to the existence of ferrite phase [23]. As ferrite concentration increases to $x = 0.3$ and 0.4 , negative curvature of ferroelectric hysteresis loops reveals the contribution of leakage current to the dielectric properties of composites, indicating lower electric resistivity of composites. It is also worthy noting that the $2P_r$ values of the composites increase with increasing ferrite concentration, and when $x = 0.3$ and 0.4 , the $2P_r$ values even exceed that of the pure BST ceramic. The similar results are found that the P_r value of the composites $(1-x)[0.94\text{Bi}_{0.5}\text{Na}_{0.5}\text{TiO}_3-0.06\text{BaTiO}_3]-x\text{CoFe}_2\text{O}_4$ ceramics with $x = 0.3$ is larger than those with $x = 0.1$ and 0.2 [19], and the P_r value of the $(1-x)\text{BaTiO}_3-x\text{CoFe}_2\text{O}_4$ thick film with $x = 0.4$ is larger than that with $x = 0.2$ [22]. In this paper, the enhanced ferroelectricity of the composites may be

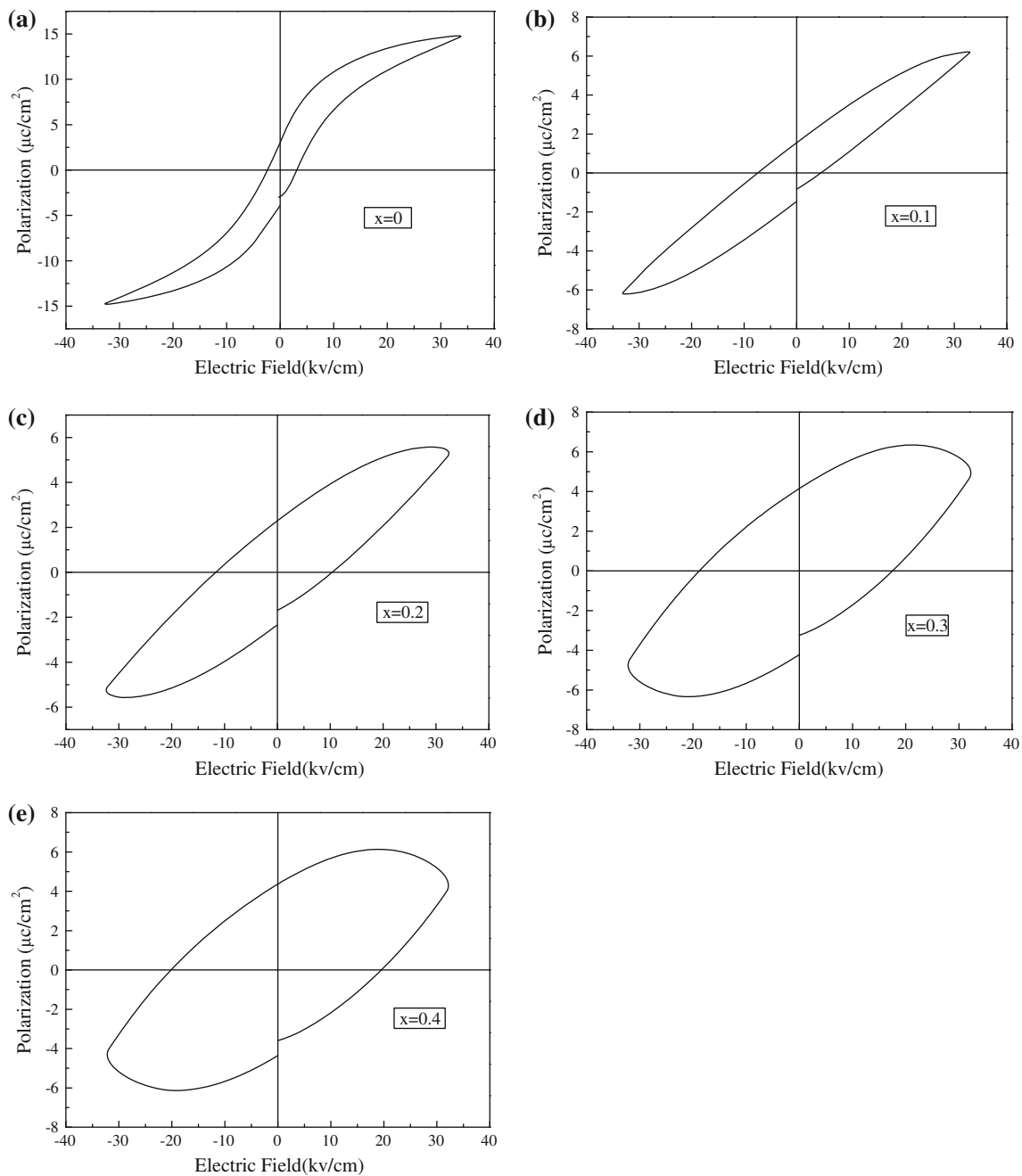


Fig. 10 The ferroelectric hysteresis loops of the $(1-x)\text{BST}-x\text{CFO}$ composites with $x = 0-0.4$. **a** $x = 0$, **b** $x = 0.1$, **c** $x = 0.2$, **d** $x = 0.3$ and **e** $x = 0.4$

attributed to above-mentioned space charge contribution in the composites [24]. With increasing ferrite concentration, the contribution of space charge in the composites to ferroelectricity is strengthened. In addition, the enclosed areas of hysteresis loops for the composites with $x = 0.1-0.4$ increase with increasing ferrite concentration, indicating the dielectric loss increases with the increase in ferrite concentration, which is in accordance with the results as shown in Fig. 5b.

4 Conclusion

The $(1-x)\text{Ba}_{0.8}\text{Sr}_{0.2}\text{TiO}_3-x\text{CoFe}_2\text{O}_4$ ceramic composites ($x = 0.1-0.4$) displaying ferromagnetic and ferroelectric and good dielectric properties simultaneously were prepared by standard solid state reaction method. XRD shows the composites are composed of tetragonal perovskite $\text{Ba}_{0.8}\text{Sr}_{0.2}\text{TiO}_3$ phase and cubic spinel CoFe_2O_4 phase. The influences of different ferrite concentration on the

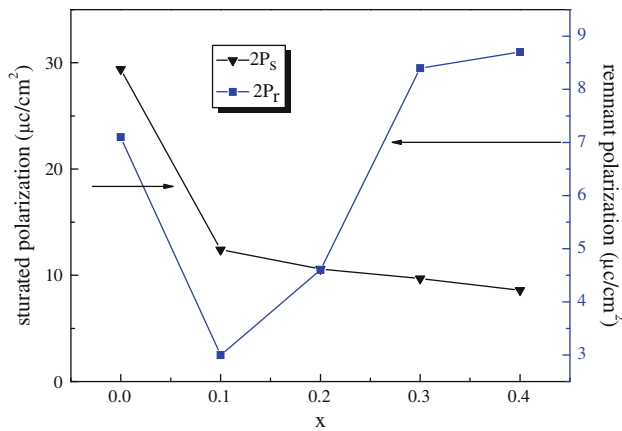


Fig. 11 CFO concentration dependence of the remanent and saturated polarization for composites

dielectric, ferromagnetic and ferroelectric properties for the composites were investigated. The variations of dielectric constant and dielectric loss at low frequency show dielectric dispersion, which can be explained on the basis of Maxwell–Wagner interfacial polarization theory. The dielectric constant values of composites with $x = 0.1$ – 0.4 are 1498.2, 966.5, 601.0, and 384.6 at 1 MHz and room temperature, respectively. The composites behave as relaxor ferroelectrics. The saturated magnetization values of the composites increase almost linearly with increasing ferrite concentration. The saturated polarization values of the composites decrease with ferrite concentration increasing, while the remnant polarization values increase with increasing ferrite concentration. The enhanced ferroelectricity of composites may be attributed to space charge contribution in the composites.

Acknowledgments This work is supported by the National Natural Science Foundation of China under Grant No. 60971008 and the Specialized Research Fund for the Doctoral Program of Higher Education of China (No. 200804870071). The authors specially acknowledge Analytical and testing Center of Huazhong University of Science and Technology for providing the great assistance.

References

1. C.W. Nan, Phys. Rev. B **50**, 6082 (1994)
2. W. Eerenstein, N.D. Mathur, J.F. Scott, Nat. (Lond.) **442**, 759 (2006)
3. J.P. Zhou, Z.C. Qiu, P. Liu, Mater. Res. Bull. **43**, 3514 (2008)
4. H. Zheng, J. Wang, S.E. Lofland, Z. Ma, L. Mohaddes-Ardabili et al., Science **303**, 661 (2004)
5. Q.H. Jiang, Z.J. Shen, J.P. Zhou, Z. Shi, C.W. Nan, J. Eur. Ceram. Soc. **27**, 279–284 (2007)
6. N. Cai, J. Zhai, C.W. Nan, Y. Lin, Z. Shi, Phys. Rev. B **68**, 224103 (2003)
7. S.K. Rout, J. Bera, in *Ferroelectrics and Dielectrics*, ed. by A.P. Tandon (Allied, New Delhi, 2004), pp. 3–7
8. D.R. Patil, B.K. Chougule, J. Alloy. Compd. **458**, 335–339 (2008)
9. J.Y. Zha, N. Cai, L. Liu, Y.H. Lin, C.W. Nan, Mater. Sci. Eng. B **99**, 329 (2003)
10. C.M. Kanamadi, J.S. Kim, H.K. Yang, B.K. Moon, B.C. Choi, J.H. Jeong, J. Alloy. Compd. **481**, 781–785 (2009)
11. C.M. Kanamadi, B.K. Das, C.W. Kim, D.I. Kang, H.G. Cha, E.S. Ji et al., Mater. Chem. Phys. **116**, 6–10 (2009)
12. K. Patankar, S. Joshi, B. Chougule, Phys. Lett. A **346**, 337 (2005)
13. C.G. Koops, Phys. Rev. **83**, 121 (1951)
14. J.C. Maxwell, *Electricity and Magnetism* (Oxford University Press, London, 1973)
15. K.W. Wagner, Ann. Phys. **40**, 817 (1993)
16. B. Parvatheeswara Rao, K.H. Rao, K. Trinadh, O.F. Calfun, J. Optoelectronic. Adv. Mater. **6**(3), 951 (2004)
17. J.X. Zhang, J.Y. Dai, H.L.W. Chan, J. Appl. Phys. **107**, 104105 (2010)
18. X.M. Chen, Y.H. Tang, I.W. Chen, Z.C. Xu, S.Y. Wu, J. Appl. Phys. **96**, 6520 (2004)
19. L.H. Pang, W.J. Ji, Y. Zhang, L. Wang, S.T. Zhang, Z.L. Luo, Y.F. Chen, J. Phys. D: Appl. Phys. **42**, 045304 (2009)
20. J.H. Yin, J. Ding, B.H. Liu, X.S. Miao, J.S. Chen, Appl. Phys. Lett. **88**, 162502 (2006)
21. X.L. Zhong, J.B. Wang, M. Liao, G.J. Huang, S.H. Xie, Y.C. Zhou, Y. Qiao, J.P. He, Appl. Phys. Lett. **90**, 152903 (2007)
22. L. Zhang, J.W. Zhai, W.F. Mo, X. Yao, Solid State Sci. **13**, 321–325 (2011)
23. W. Chen, Z.H. Wang, W. Zhu, O.K. Tan, J. Phys. D Appl. Phys. **42**, 075421 (2009)
24. R.Y. Zheng, J. Wang, S. Ramakrishna, J. Appl. Phys. **104**, 034106 (2008)